Proceedings of the 10th International Pipeline Conference
IPC2014
September 29 – October 03, 2014, Calgary, Alberta, Canada

IPC2014-33323

STRUCTURAL PERFORMANCE OF BURIED STEEL PIPELINES CROSSING STRIKE-SLIP FAULTS

Polynikis Vazouras
Department of Civil Engineering,
Univ. of Thessaly, Volos, Greece

Panos Dakoulas
Department of Civil Engineering,
Univ. of Thessaly, Volos, Greece

Spyros A. Karamanos
Department of Mechanical Engineering,
Univ. of Thessaly, Volos, Greece
email:skara@mie.uth.gr

ABSTRACT

The performance of pipelines subjected to permanent strike-slip fault movement is investigated by combining detailed numerical simulations and closed-form solutions. A closed-form solution for the force-displacement relationship of a buried pipeline subjected to tension is presented and used in the form of nonlinear springs at the two ends of the pipeline in a refined finite element model, allowing an efficient nonlinear analysis of the pipe-soil system at large strike-slip fault movements. The analysis accounts for large deformations, inelastic material behaviour of the pipeline and the surrounding soil, as well as contact and friction conditions on the soil-pipe interface. Appropriate performance criteria of the steel pipeline are adopted and monitored throughout the analysis. It is shown that the end conditions of the pipeline have a significant influence on pipeline performance. For a strike-slip fault normal to the pipeline axis, local buckling occurs at relatively small fault displacements. As the angle between the fault normal and the pipeline axis increases, local buckling can be avoided due to longitudinal stretching, but the pipeline may fail due to excessive axial tensile strains or cross sectional flattening.

INTRODUCTION

Ground-induced actions due fault movements are responsible for significant damages in oil and gas buried steel pipelines. Those deformations are applied in a quasi-static manner, and are not necessarily associated with high seismic intensity, but the pipeline may be seriously deformed, well beyond the elastic range of pipe material and may cause pipeline failure; high tensile stresses may cause fracture of the pipeline wall, especially at welds or defected locations or welds, whereas compressive stresses may cause buckling, in the form of pipe wall wrinkling, also referred to as “local buckling” or “kinking”.

The pioneering work of Newmark and Hall [1] has been extended by Kennedy et al.[2], Wang and Yeh[3], Wang and Wang [4]and Takada et al. [5] through a beam-type approach for describing pipeline deformation. More recent works on this subject have been reported by Karamitros et al. [6] Liu et al. [7]and Trifonov&Cherniy[8]. In addition to the above analytical and numerical studies, notable experimental works on the effects of strike-slip faults on buried high-density polyethylene (HDPE) pipelines have been reported in series of recent papers by Ha et al. [9] and Abdoun et al. [10].The analytical works outlined above have modelled soil conditions based on a spring-type approach. A more rigorous approach has been followed in most recent papersof the present authors [11] [12], for buried steel pipelines crossing strike-slip faults at various angles with respect to the fault plane, through a finite element modelling of the soil-pipeline system, which accounts rigorously for the inelastic behaviour of the surrounding soil, the interaction and the contact between the soil and the pipe (including friction contact and the development of gap), the development of large inelastic strains in the steel pipeline, the distortion of the pipeline cross-section and the possibility of local buckling, the presence of internal pressure.

The objective of the present paper is to develop a refined numerical model, extending the work presented in [11][12] and accounting for appropriate end effects, to investigate the mechanical behavior of underground steel pipelines crossing oblique strike-slip faults subjected to permanent ground movement. Towards this purpose, the rigorous numerical methodology developed in the previous publications is

combined with a new closed-form mathematical solution of equivalent nonlinear springs at the model ends, allowing for efficient and accurate simulation of pipeline behavior.

NUMERICAL MODEL DESCRIPTION

The mechanical behavior of a steel pipeline crossing a strike-slip fault is simulated using finite element program ABAQUS [13]. Relative ground displacement *d* is applied in a direction that forms an angle β with the normal on the pipeline direction, as shown schematically in Figure 1, ranging from zero to 45 degrees.

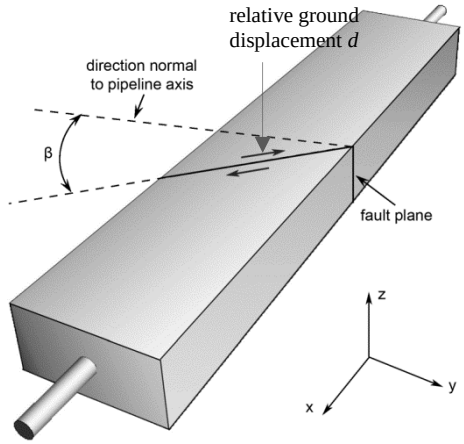

Figure 1.Schematic representation of buried pipeline subjected to oblique strike-slip fault displacement.

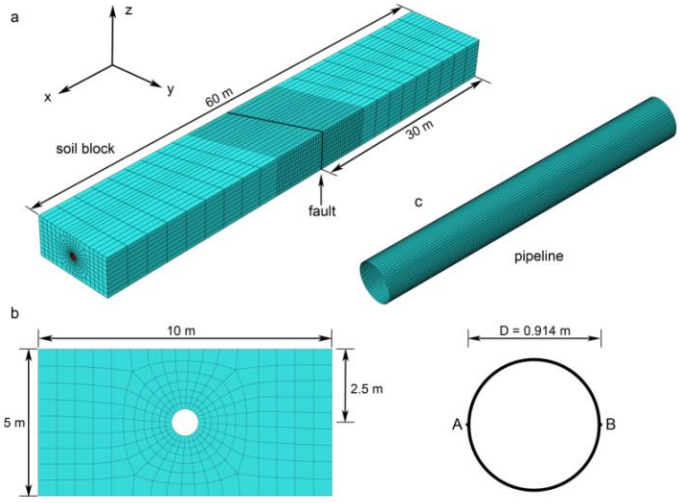

Figure 2.Finite element model for angle β equal to 25°: Finite element discretization of the (a) soil prism with tectonic strike-slip fault (b) soil prism cross-section and (c) the steel pipeline.

Figure 2 shows a numerical model for the soil-pipeline system; its size and discretization is similar to the model employed in [11] [12]. It consists of a soil prism having dimensions 60 × 10 ×5 pipe diameters. The angle between the fault plane and the normal on the pipeline axis in the model shown in Figure 2 is equal to β =25° but different values of β can be also assumed.

The fault movement is considered to occur within a narrow transverse zone of width *w*, a common practice in several recent numerical studies of fault-foundation interaction [14][15], also corresponding to a more realistic representation of the fault displacement mechanism. A relevant numerical investigation in [11] has shown that a value of *w* equal to 0.33m is adequate for the purposes of the present analysis.

Figure 2b shows the soil finite element mesh in the y-z plane and Figure 2c depicts the corresponding mesh for the steel pipe. Four-node reduced-integration shell elements (type S4R) are employed for modeling the cylindrical pipeline segment, and eight-node reduced-integration "brick" elements (C3D8R) are used to simulate the surrounding soil. The burial depth is chosen equal to about 2 times of pipe diameter, which is in accordance with pipeline engineering practice [16]. The prism length in the x direction is equal to more than 65 pipe diameters, whereas dimensions in directions y and z are equal to 11 and 5 times the pipe diameter, respectively.

The central part of the pipeline model, where maximum stresses and strains are expected, consists of a finermesh. A total of 54 shell elements around the cylinder circumference in this central part have been found to be adequate to achieve convergence, whereas the size of the shell elements in the longitudinal direction has been chosen equal to 1/26 of the pipeline outer diameter *D*. This mesh has been shown capable of describing the formation of short-wave wrinkling (local buckling) on the pipeline wall [11]. The mesh chosen for the pipe segments far from the fault location is coarser. Similarly, the finite element mesh for the soil is more refined in the region near the fault and coarser elsewhere.

A large-strain von Misses plasticity model with isotropic hardening is employed for the steel pipe material. The mechanical behavior of soil material is described through an elastic-perfectly plastic Mohr-Coulomb constitutive model.

The analysis is conducted by applying gravity firstand, subsequently, using a displacement-controlled scheme, in which the fault displacement *d* is increased gradually. The base and vertical-boundary nodes of the first soil block remain fixed in the horizontal direction, whereas the corresponding nodes of the second soil block are subject to a uniform displacement,in a direction parallel to the fault plane. Finally in order to incorporate infinite length in x direction for both the pipe and the soil a closed-form mathematical solution is presented below. The equivalent nonlinear spring derived from this solution is attached at both ends of the pipe accounting for infinite model length. One free end of the nonlinear spring remained fixed while the other moved according to fault direction

NONLINEAR SPRING FOR INFINITELY LONG PIPELINE IN TENSION

A pipeline segment is considered with diameter D, thickness t, length L_a, made of a material having Young's

Modulus E and Poisson's ratio *v*. The pipeline is buried in a soil with density ρ_s, cohesion c, friction angle ϕ,Young's Modulus E_s and Poisson's ratio v_s(Figure 3a). The pipeline issubjected to a pullout force at the near end, while keeping fixed the far end (Figure 3b). The fixed far end of the pipeline may be at an infinite distance ($L_a = \infty$) which is the most common case in real applications.

It should be noted that in a pullout test, nonlinearity will occur first at the pipe-soil interface at which the value of shear strength is quite lower than the yield stress of soil. Thus, the soil will behave elastically, even at very high pullout forces, at which the pipeline material may yield.

As shown in Figure 3b, when the applied displacement u_0 at the near end exceeds a critical value, part of the pipeline along a distance L_s experiences sliding at its interface, whereas the rest of the infinitely long pipeline remains "bonded" to the soil that behaves elastically. In the following, pipeline response in the non-sliding and sliding parts is analyzed.

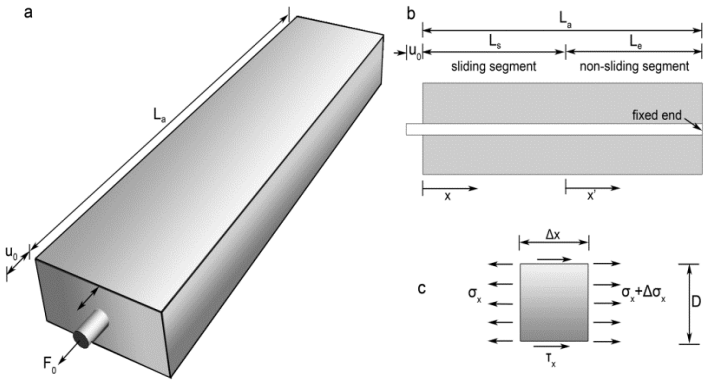

Figure 3: Buried pipeline subjected to tension (a) perspective view (b) vertical section and (c) free body diagram of pipeline segment. The total length L_a may be either infinite or finite.

Elastic behavior (non-sliding interface)

Figure 3c illustrates a segment of the pipeline subjected to tensile and shear stresses. For shear stress at the pipe interface $\tau \le \tau_{\max}$,the mobilized value of τ is equal to

$$\tau = k_s\, u \tag{1}$$

Considering the axial force change dF along the pipeline of length dx

$$dF = -\pi D\tau dx = -\pi D k_s\, u dx \tag{2}$$

and using the stress-strain relationship,

$$\frac{dF}{dx} = \frac{d}{dx}(EA\varepsilon) = -EA\frac{d^2u}{dx^2} \tag{3}$$

the equilibrium equation for the pipesegment becomes

$$EA\frac{d^2u}{dx^2} - \pi D k_s\, u = 0 \tag{4}$$

Equation (4)may be written as

$$\frac{d^2u}{dx^2} - \lambda^2\, u = 0 \tag{5}$$

where

$$\lambda = \sqrt{\frac{\pi D k_s}{EA}} \tag{6}$$

The solution of equation (5) is given by

$$u = C_1 e^{-\lambda x} + C_2 e^{\lambda x} \tag{7}$$

For $x \to \infty$, $u = 0$ and therefore $C_2 = 0$, whereas for $x = 0$, $u(0) = u_0 = C_1$. The axial force along the pipe is equal to

$$F(x) = -EA\frac{du}{dx} = \lambda EAu = \lambda EA\, u_0\, e^{-\lambda x} \tag{8}$$

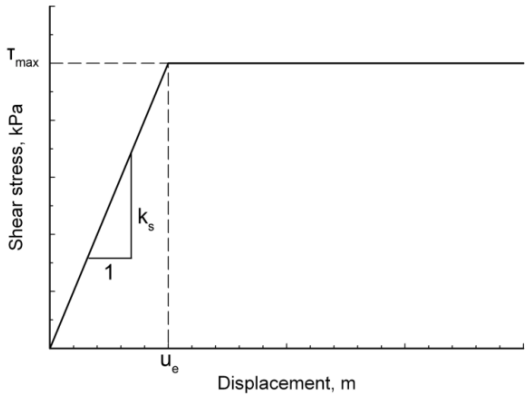

Figure 4.Shear stress-displacement relationship at the pipe-soil interface.

For the limit case at which sliding initiates at x=0, the displacement $u(0) = u_0$ becomes equal to the elastic limit displacement $u_e = \tau_{\max} / k_s$ (Figure 4). Thus, the axial force at x=0 can be written as

$$F_0 = \lambda EA\frac{\tau_{\max}}{k_s} \tag{9}$$

Hence, for linear elastic response, the *equivalent linear spring*constant for an infinitely long pipeline subjected to tension is given by

$$K_t = \lambda EA \tag{10}$$

Inelastic behavior (sliding interface)

When the pipeline is subjected to a pullout displacement $u_0 > u_e = \tau_{\max} / k_s$, a segment of the pipeline slides along a distance L_s, whereas the rest of the pipeline interface behaves

elastically. For the sliding segment, taking the equilibrium of a pipe element (Figure 3c) leads to

$$EA\frac{d^2u}{dx^2} - \pi D\tau_{\max} = 0 \quad (11)$$

or

$$\frac{d^2u}{dx^2} = m \quad (12)$$

where

$$m = \frac{\pi D\tau_{\max}}{EA} \quad (13)$$

The axial strain decreases linearly with the distance x and may be written as

$$\varepsilon(x) = -\frac{du}{dx} = -mx + C_3 \quad (14)$$

For $x = 0$, the axial strain is equal to

$$\varepsilon(0) = \varepsilon_0 = -\left.\frac{du}{dx}\right|_{x=0} = C_3 \quad (15)$$

whereas for $x = L_s$, it becomes equal to the elastic limit strain

$$\varepsilon(L_s) = \varepsilon_e = -\left.\frac{du}{dx}\right|_{x=L_s} = -mL_s + \varepsilon_0 \quad (16)$$

Integrating $\varepsilon(x)$ from $x = 0$ to L_s, the displacement difference $u_0 - u_e$ is found equal to

$$u_0 - u_e = \frac{1}{2}(\varepsilon_0 - \varepsilon_e)L_s + \varepsilon_e L_s = \frac{1}{2}mL_s^2 + \varepsilon_e L_s \quad (17)$$

From(17), the length L_s is equal to

$$L_s = \frac{1}{m}\left(\sqrt{\varepsilon_e^{\,2} + 2m(u_0 - u_e)} - \varepsilon_e\right) \quad (18)$$

Substituting the maximum elastic strain obtained from the non-sliding side of the pipeline

$$\varepsilon_e = \lambda u_e = \lambda\frac{\tau_{\max}}{k_s} \quad (19)$$

equation (18) becomes

$$L_s = \frac{1}{m}\left(\sqrt{\left(\lambda\frac{\tau_{\max}}{k_s}\right)^2 + 2m\left(u_0 - \frac{\tau_{\max}}{k_s}\right)} - \lambda\frac{\tau_{\max}}{k_s}\right) \quad (20)$$

Equations for equivalent nonlinear spring

The force at the pipe end is given by

$$F_0 = \pi D\tau_{\max}L_s + \lambda EAu_e \quad (21)$$

Considering the above analysis, from equations (9), (20) and (21), the force–displacement ($F_0 - u_0$) relation for an infinitely long pipe becomes:

- for

$$u_0 \le \frac{\tau_{\max}}{k_s},$$

$$F_0 = \lambda EAu_0 \quad (22)$$

- for

$$u_0 > \frac{\tau_{\max}}{k_s},$$

$$F_0 = \lambda EA\frac{\tau_{\max}}{k_s} + \frac{\pi D\tau_{\max}}{m}\left(\sqrt{\left(\lambda\frac{\tau_{\max}}{k_s}\right)^2 + 2m\left(u_0 - \frac{\tau_{\max}}{k_s}\right)} - \lambda\frac{\tau_{\max}}{k_s}\right) \quad (23)$$

PERFORMANCE CRITERIA FOR STRAIN-BASED DESIGN OF BURIED STEEL PIPELINES

Under strong permanent ground-induced actions, buried steel pipelines exhibit severe deformation beyond the elastic limit. Steel material is quite ductile and capable of sustaining significant amount of inelastic deformation, but at locations where large tensile strains develop, rupture of the pipeline wall may occur. Wrinkling (local buckling) of pipeline wall may also occur due to excessive compression at the pipeline wall, followed by pipe wall folding and development of significant local strains. Furthermore, severe distortions of the pipeline cross-section may render the pipeline non-operational. To quantify the amount of damage in a buried pipeline under severe ground-induced action, the following three performance criteria are monitored in the present analysis [12]:

- tensile strain equal to 3% and 5% in the longitudinal direction of the pipeline, which may cause pipe wall rupture,
- local buckling (wrinkling) formation, and
- excessive distortion of the pipeline cross-section so that the "flattening parameter" f ,defined $f = \Delta D/D$ (ΔD is the change of pipe diameter in the flattening direction), reaches a value of 0.15.

During the consecutive stages of fault displacement application, the performance criteria are evaluated, monitoring the maximum values of longitudinal strain along the pipeline, as well as the cross-sectional distortion (flattening) at various cross-sections. Furthermore, the finite element model is capable of simulating rigorously the formation of pipeline wall wrinkling.

NUMERICAL RESULTS FOR PIPELINES CROSSING STRIKE-SLIP FAULTS

In this section, numerical results are obtained for the 36-inch X65 buried pipeline that crosses strike-slip faults at different angles, with thickness equal to 9.5 mm (3/8 in), so that *D/t* is equal to 96. Three crossing angles were investigated with

zero internal pressure using the numerical model described above. The yield stress σ_y and ultimate stress σ_u are equal to 450 MPa (65 ksi) and 560 MPa (81.2 ksi), respectively, with a 30% elongation at the ultimate stress (ε_u = 0.3).Infinite pipeline length is assumed. The pipeline is buried in the cohesive soil, under "undrained" conditions, having a density ρ_s =2000 kg/m^3, cohesion c =50 kPa, friction angle ϕ =0°,Young's Modulus E_s =25 MPa and Poisson's ratio ν_s =0.5.

Pipeline performance for fault angle $\beta = 0^\circ$

Using the numerical model, Figure 5a and Figure 5b plot the distribution of axial strain at the tension and compression sides of the pipeline respectively, for different values of fault displacement d . Figure 5c shows the evolution of pipeline stress state and deformation at a stage just before local buckling, and immediately after buckling. Considering the convention for local buckling onset in which significant distortion of the cross-section occurs due to the development of a localized wrinkling pattern on the pipe wall, on the compression side of the deformed pipeline, as stated in [11][12], local buckling occurs at a fault displacement of about d_{cr} =0.43 m; this is the most critical performance criterion for the present case. The 3% tensile strain is reached at d_{cr} =1.13 m, whereas the critical flattening occurs at about 1.96 m. Note that both of these criteria are reached at the buckled location well beyond the formation of the buckle. The 5% tensile strain performance criterion is not reached within the maximum fault displacement (4 m) considered in the analysis; in fact, the tensile strain reaches a value of about 4.1% in the course of this analysis.

Pipeline performance for fault angle $\beta = 25^\circ$

Figure 6a plots the deformed shape of the pipeline and the distribution of the axial strain at fault displacements equal to d =1, 1.5, 2 and 2.5 m. In this case, additional pipeline extension, equal to $d \sin\beta$, occurs, resulting in significant reduction of the compressive bending strains, and preventing the development of local buckling.

Figure 6b illustrates the ovalization of the pipe cross-section at the fault location ($x = 0$). The critical fault displacement for ovalization (flattening) given in Table 1 is 1.28 m. Hence, the deformed pipeline shapes at $d \geq$ 1.5 m, shown in Figure 6b, have already exceeded the ovalization performance criterion. Figure 7 plots the distribution of displacement in the longitudinal x direction at generators A and B (shown in Figure 2) of the pipeline in terms of the distance from the fault, for fault displacements d =1, 1.5, 2 and 2.5 m. It is evident that the movement along the generators varies due to bending for x <10 m, but it is practically identical for x >10 m, indicating that, outside the most-strained region near the fault, the pipeline is practically under pure axial tension.

Table 1. Critical fault displacement for various performance criteria with respect to fault angle β

Fault angle β	Critical fault displacement, m			
	Local buckling	Flattening	Strain 3%	Strain 5%
β=0°	0.43	1.96	1.13	>4.00*
β=25°	None	1.28	1.73	2.17
β=45°	None	1.12	1.08	1.40

* Not reached within a maximum fault movement of d=4 m

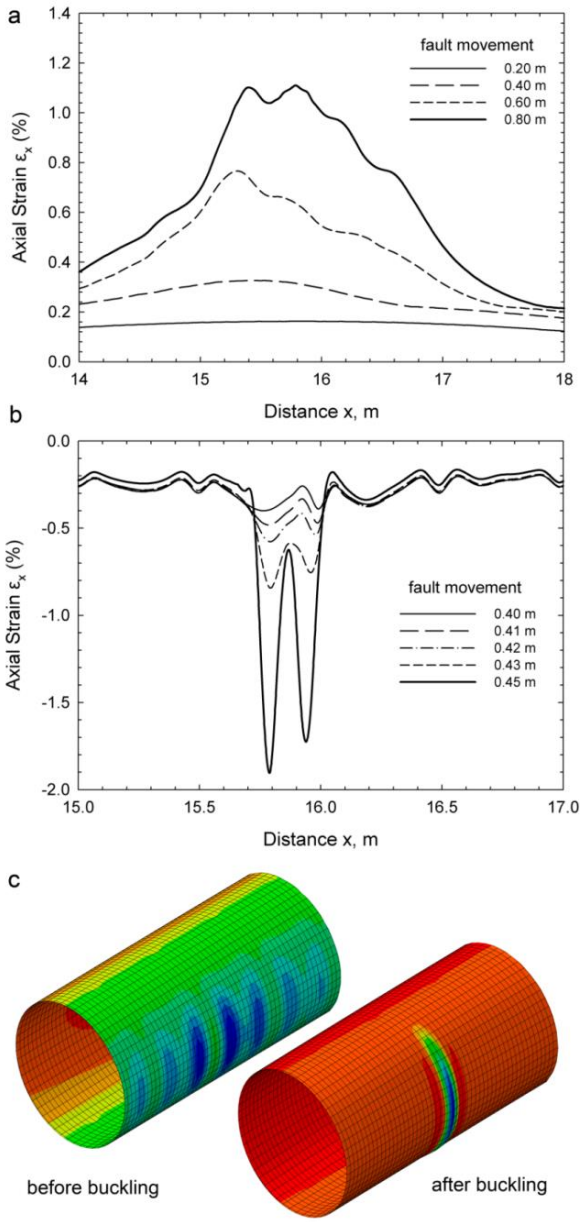

Figure 5.(a) Axial strain along the pipeline side under tension (b) axial strain along the pipeline side under compression (c) pipeline shape at critical location before and after buckling. (angle β=0°).

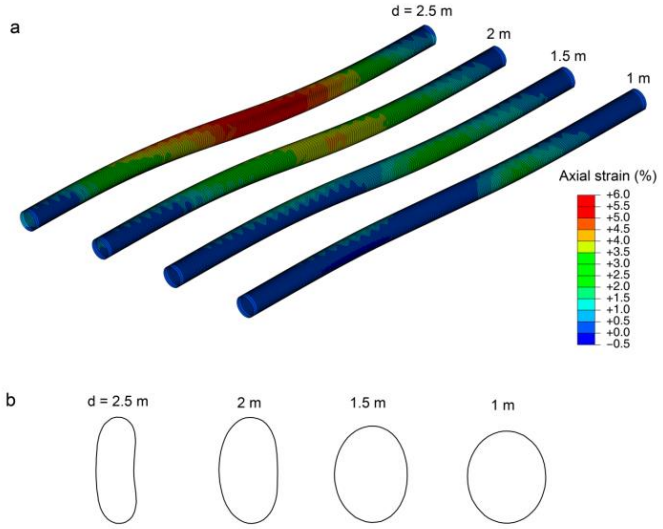

Figure 6. Finite element results from model withβ=25°:(a) Axial strain and (b) pipeline section deformation at $d = 1$, 1.5, 2 and 2.5 m.

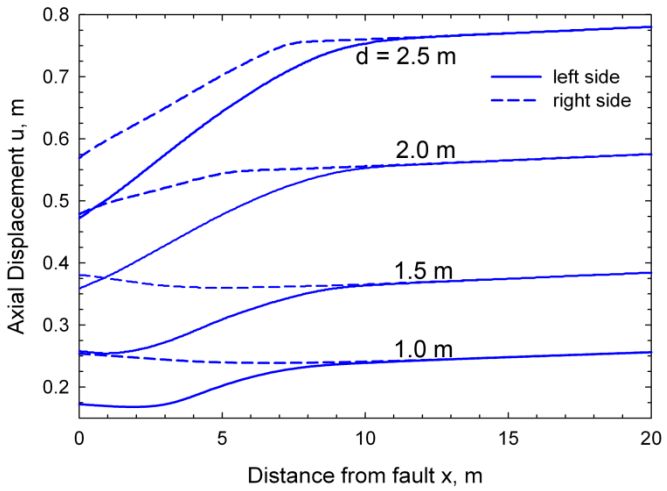

Figure 7. Distribution of axial displacement at the outer generators located at the left and right side of the pipeline versus the distance from the fault, (β=25°).

Pipeline performance for fault angle $\beta = 45^{\circ}$

For a fault angle $\beta = 45^{\circ}$, the pipeline is subjected to substantial extension during fault movement in the x direction by $d \sin\beta$ .In this case, local buckling does not occur, but the other performance criteria are reached at much smaller fault displacement values (Table 1). Flattening occurs at 1.12m, whereas the 3% and 5% tensile axial strain criteria at 1.08m and 1.40m, respectively.

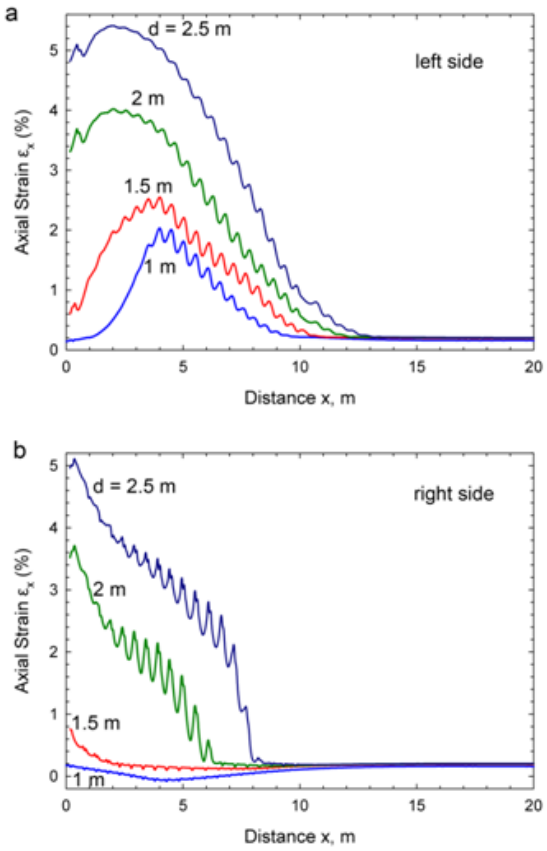

Figure 8. Distribution of axial strain versus distance from the fault, (β=25°) along generator at the (a) left side and (b) right side of the pipeline.

Effect of fault angle on pipeline performance

The above numerical results for the X65-steel infinite length pipeline with zero pressure are summarized in graphical form in Figure 10, where the fault displacement values corresponding to the performance criteria under consideration, are plotted with respect to the crossing angle β . The results indicate that for non-positive and small positive (less than 5°) values of β , local buckling is the dominant limit state. For greater values of β , two major limit states, namely the 3% longitudinal tensile strain and the cross section flattening are most important. Under increasing angle β, the normalized ultimate displacement for cross-sectional distortion remains the same, whereas 3% and 5% of tensile strain decrease. Figure 11 plots the performance criteria for the same pipeline embedded in the same soil conditions but having now internal pressure. It is obvious that with internal pressure no ovalization is observed.

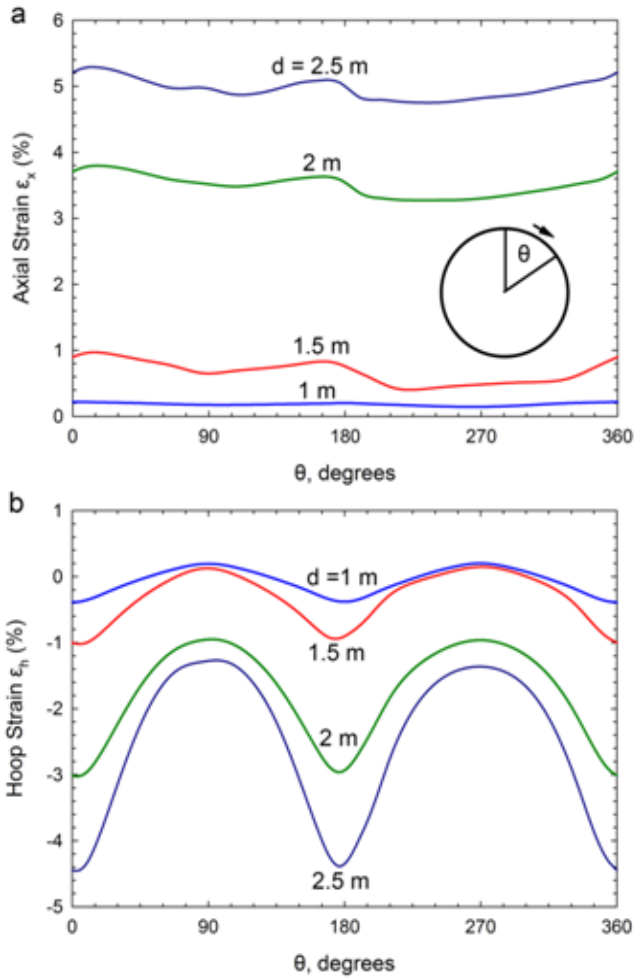

Figure 9. Distribution of (a) axial strain and (b) hoop strain around the perimeter of the pipeline section at $x = 0$, (crossing angle β equal to 25°).

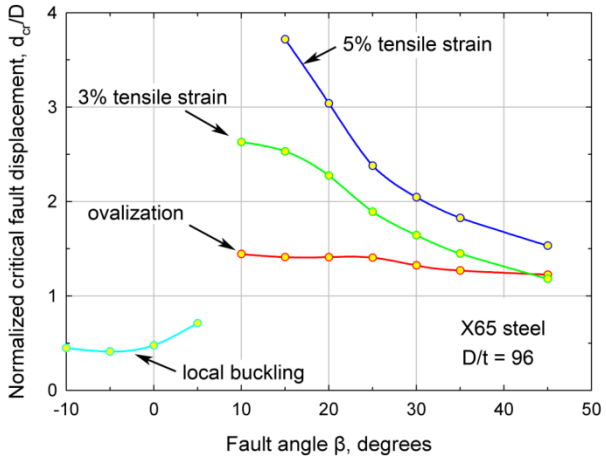

Figure 10: Normalized critical fault displacement for various performance limits at different angles of β and infinite pipeline length (X65, D/t=96, Clay I, p=0).

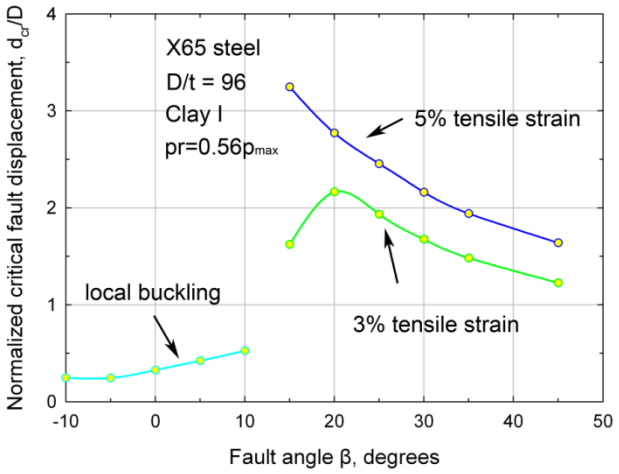

Figure 11: Normalized critical fault displacement for various performance limits at different angles of β for a pipeline of infinite length (X65, D/t=96, Clay I, p=0.56p_{max})

CONCLUSIONS

The pipe-soil interaction and the performance of pipelines subjected to permanent strike-slip fault movement have been investigated using refined models that combine detailed numerical simulations and mathematical solutions. A closed-form mathematical solution for the force-displacement relationship of a buried pipeline subjected to tension has been developed for pipelines. The closed-form solution accounts for the elastic deformation of the soil and pipe, and the development of sliding, when the shear stress at the pipe-soil interface reaches its shear strength. The closed-form solution enables the consideration of nonlinear springs at the two ends of the pipeline in a refined finite-element formulation, allowing for an efficient nonlinear analysis of the pipe-soil interaction problem at large strike-slip fault movements. The numerical study is based on a large number of refined numerical models corresponding to various values of angle β between the pipeline axis and the direction normal to the fault plane.

The main conclusions of the study can be summarized as follows:

1. The proposed nonlinear force-displacement relationships allow for an efficient, refined numerical simulation of the soil-pipe interaction during large permanent fault movements, through the use of nonlinear springs in finite element models that describe the pipe-soil system in a rigorous manner.
2. Numerical simulations of X65 pipelines with D/t=96 buried in clay soil crossing strike-slip faults normal to their pipeline axis ($\beta = 0^\circ$) have shown that local buckling of pipe wall occurs at small fault displacements.

3. Upon development of local buckling during seismic fault movement, the location of maximum flattening and axial strain is at the buckled cross-section.
4. For values of β greater than 15°, local buckling does not occur due to pipeline stretching that reduces the compressive stresses caused by bending. Thus, if practically feasible, aligning the pipeline so that it forms a positive value of β that is just large enough to avoid local buckling, may improve pipeline performance, allowing larger critical fault displacements for the flattening or tensile strain criteria.
5. As tension in the pipeline increases with increasing values of the angle β, the critical fault displacement corresponding to the flattening performance criterion and, most importantly, to the 3%- and 5%-tensile strain criteria decrease.

The methodology in the present paper is applied to simulate the behavior of pipelines crossing strike-slip faults, but can be also applicable to other types of permanent ground-induced actions, such as normal and reverse faults, as well as to buried pipelines subjected to other types of ground-induced action (landslides, differential settlement or lateral spreading).

NOMENCLATURE

A	:	pipeline cross-sectional area
c	:	cohesion of soil
D	:	outer pipe diameter
d	:	fault displacement
D/t	:	pipe outer diameter-to-thickness ratio
E	:	Young's modulus
F_0	:	Axial force at x=0
k_s	:	shear stiffness of pipe-soil interface
K_t	:	equivalent linear spring constant
L_e	:	non-sliding pipeline segment
L_s	:	sliding pipeline segment
p	:	pipe internal pressure
p_{max}	:	maximum pipe pressure
t	:	pipe wall thickness
u	:	axial pipeline displacement
w	:	fault width
β	:	fault angle with respect to normal to pipe axis
ε	:	axial strain on pipe wall
ν	:	Poisson's ratio
ρ	:	soil density
σ_y	:	pipe material yield stress
σ_u	:	pipe material ultimate stress
τ	:	shear stress at pipe-soil interface
τ_{max}	:	maximum shear stress at pipe-soil interface
φ	:	friction angle of pipe-soil interface

ACKNOWLEDGMENTS

This work was supported by a financial grant from the Research Fund for Coal and Steel of the European Commission, GIPIPE project: "Safety of buried steel pipelines under ground-indused deformations.", Grant No.RFSR-CT-2011-00027. The authors would like to thank Mr. Gregory Sarvanis for his help in preparing the manuscript.

REFERENCES

[1] Newmark N. M., Hall W. J. (1975), "Pipeline design to resist large fault displacement". *Proceedings of U.S. National Conference on Earthquake Engineering*; 416–425.

[2] Kennedy, R. P., Chow, A. W. and Williamson, R. A. (1977), "Fault movement effects on buried oil pipeline", *ASCE Journal of Transportation Engineering*, Vol. 103, pp. 617-633.

[3] Wang, L. R. L. and Yeh, Y. A. (1985), "A refined seismic analysis and design of buried pipeline for fault movement", *Earthquake Engineering &Structural Dynamics*, Vol. 13, pp. 75-96.

[4] Wang L. L. R., Wang L. J. (1995), Parametric study of buried pipelines due to large fault movement. *ASCE, TCLEE* 1995; (6):152–159.

[5] Takada, S., Hassani, N.and Fukuda, K. (2001), "A new proposal for simplified design of buried steel pipes crossing active faults", *Earthquake Engineering and Structural Dynamics*, 2001; Vol. 30, pp.1243–1257.

[6] Karamitros, D. K., Bouckovalas, G. D., and Kouretzis, G. P. (2007), "Stress Analysis of Buried Steel Pipelines at Strike-Slip Fault Crossings.",*Soil Dynamics & Earthquake Engineering*, Vol. 27, pp. 200-211

[7] Liu, M., Wang, Y.-Y., and Yu, Z., (2008), "Response of pipelines under fault crossing", *Proceedings Intern. Offshore and Polar Engineering Conference*, Vancouver, BC, Canada.

[8] Trifonov, O. V. and Cherniy, V. P. (2010), "A semi-analytical approach to a nonlinear stress–strain analysis of buried steel pipelines crossing active faults.",*Soil Dynamics & Earthquake Engineering*, Vol. 30, pp. 1298-1308.

[9] Ha, D., Abdoun T.H., O'Rourke, M.J., Symans, M.D., O'Rourke, T.D., Palmer, M.C., and Stewart, H.E. (2008), **"**Buried high-density polyethylene pipelines subjected to normal and strike-slip faulting–a centrifuge investigation**",** *Canadian Geotechnical Engineering Journal*, Vol. 45, pp. 1733-1742.

[10] Abdoun T. H., Ha, D., O'Rourke, M. J., Symans, M. D., O'Rourke, T. D., Palmer, M. C., and Stewart, H. E. (2009), "Factors influencing the behavior of buried pipelines subjected to earthquake faulting.", *Soil Dynamics and Earthquake Engineering*, Vol. 29, pp. 415–427.

[11] Vazouras, P., Karamanos, S. A., and Dakoulas, P. (2010), "Finite Element Analysis of Buried Steel Pipelines Under Strike-Slip Fault Displacements", *Soil Dynamics and Earthquake Engineering*, Vol. 30, No. 11, pp. 1361–1376.

[12] Vazouras, P., Karamanos, S. A., and Dakoulas, P. (2012), "Mechanical behavior of buried steel pipes crossing active strike-slip faults", *Soil Dynamics and Earthq. Engineering*, 41:164–180.

[13] ABAQUS (2012): *Users' Manual*, Simulia, Providence, RI, USA.

[14] Anastasopoulos, I., Callerio, A., Bransby, M. F., Davies, M. C., Nahas, A. El, Faccioli, E., Gazetas, G., Masella, A., Paolucci, R., Pecker, A., Rossigniol, E. (2008), "Numerical analyses of fault foundation interaction.", *Bulletin of Earthquake Engineering*, Springer, Vol. 6, No. 4, pp. 645-675.

[15] Gazetas, G., Anastasopoulos, I. and Apostolou, M. (2007), "Shallow and deep foundation under fault rapture or strong seismic shaking", K. Pitilakis (ed.), *Earthquake Geotechnical Engineering*, Springer, pp. 185-215.

[16] Mohitpour, M., Golshan, H. and Murray, A. (2007), *Pipeline Design & Construction: A Practical Approach*, Third Edition, ASME Press, New York, NY.